ELSEVIER

Surface Science 443 (1999) 125–132

surface science

www.elsevier.nl/locate/susc

# The decomposition of $NO_2$ on Rh(111): product NO velocity and angular intensity distributions

K.D. Gibson, J.I. Colonell, S.J. Sibener *

*The James Franck Institute and Department of Chemistry, The University of Chicago, 5640 South Ellis Avenue, Chicago, IL 60637, USA*

Received 7 July 1999; accepted for publication 16 September 1999

**Abstract**

The velocity and angular distributions of NO produced from the decomposition of $NO_2$ on Rh(111) under both reducing and oxidizing conditions have been measured at surface temperatures between 500 K and 1000 K. When a concurrent $H_2$ beam is used, which keeps the surface free of oxygen, the NO product has much more translational energy than expected for equilibration at the surface temperature, but is dependent on $T_s$. There is total energy scaling; the translational energy is independent of final angle. A small amount of $N_2$ is also produced. When the $H_2$ beam is turned off, oxygen builds up on the surface. Under this oxidizing condition, the NO product has an almost Maxwell–Boltzmann velocity distribution at the surface temperature. 

*Keywords:* Catalysis; Hydrogen; Molecule–solid reactions; Nitrogen dioxide; Rhodium; Single crystal surfaces; Surface chemical reaction

## 1. Introduction

Rhodium, a component of three-way automotive exhaust catalysts, is important because it selectively reduces $NO_x$ to $N_2$ [1,2]. Platinum and palladium also catalyze the reduction, but produce large quantities of undesirable $NH_3$ and $N_2O$. In our laboratory, we have been systematically investigating the dynamics of the $NO_x$ reduction on Rh(111). In a previous paper, we studied the $NO+H_2$/Rh(111) reaction [3]. In this paper, we report our results for the decomposition of $NO_2$.

On many transition metal surfaces, $NO_2$ readily decomposes. It is a very effective agent for quickly depositing large quantities of oxygen, particularly under ultra-high vacuum (UHV) conditions [4–6]. There have been studies investigating the adsorption and desorption of $NO_2$ from Pt [7,8], Pd(111) [9], and Ru(001) [10]. These involved dosing the crystals at cryogenic temperatures. On Pt(111), the co-adsorption of $NO_2$ and oxygen was also studied [11]. When the Pt(111) crystal is exposed to $NO_2$ at 100 K and then heated, the $NO_2$ completely decomposes to NO and oxygen. At larger coverages, some of the $NO_2$ desorbs. High-resolution electron energy loss spectroscopy (HREELS) showed that the $NO_2$ is adsorbed as a μ-N,O-nitrito surface complex (bound to the surface through the N and one O atoms) [11]. When the surface is pre-covered with oxygen atoms, most of the $NO_2$ is reversibly adsorbed. HREELS spectra also indicated that the $NO_2$ is nitro-bonded (bound to the surface through the N atom only). On an initially clean Pd(111) surface, the behavior is similar to that of Pt(111), and the $NO_2$ is also

* Corresponding author. Fax: +1-773-7025863.
*E-mail address:* s-sibener@uchicago.edu (S. Sibener)

0039-6028/99/$ - see front matter 
PII: S0039-6028(99)00993-0

adsorbed as a μ-N,O-nitrito complex. On Ru(001), some of the $NO_2$ dissociates to NO and O even at 80 K, and any $NO_2$ in the first layer are adsorbed only through the N atom. Also, the initial decomposition of the $NO_2$ inhibits any further decomposition. The trend is that the presence of oxygen on the surface changes the adsorption geometry and suppresses the decomposition of $NO_2$.

In our laboratory, the kinetics of $NO_2$ decomposition on Rh(111) have been studied [12]. When a Rh(111) crystal [surface temperature ($T_s$) = 525 K] is exposed to a room temperature $NO_2$ beam, oxygen is very quickly deposited on the surface, ~50 times faster than with an equivalent $O_2$ beam. The reaction products are principally gas phase NO and adsorbed (and absorbed) oxygen. Temperature programmed desorption (TPD) experiments show that for equivalent quantities of deposited oxygen, the $O_2$ desorption peak due to absorbed oxygen occurs at a higher temperature when the surface was dosed with $NO_2$ rather than $O_2$ [13].

Using our ability to measure the velocity of reaction products under steady-state conditions, we studied the dynamics of $NO_2$ decomposition on the Rh(111) surface. The reaction was studied at elevated temperatures, where practical $NO_x$ reduction catalysts operate. This contrasts with, and offers many advantages over, previous investigations where reactants were typically deposited at cryogenic surface temperatures, and the reactions studied under non-steady state conditions during which the catalyst's temperature was subsequently ramped up to reach threshold temperatures suitable for reaction. We performed experiments both when there was a concurrent $H_2$ beam (reducing conditions) and when the oxygen was allowed to accumulate on the surface.

## 2. Experimental

These experiments were performed in a scattering machine thoroughly described elsewhere [14,15]; only the essential features will be mentioned here. The UHV scattering chamber has a differentially pumped quadrupole mass spectrometer with an angular resolution of 1°. Attached to the detector housing, and rotating with it, is a double-differentially pumped housing containing an AC hysteresis motor for driving a post-crystal chopper, which allows us to make time-of-flight (TOF) measurements of desorbing molecules. This has a 511 channel cross-correlation pattern, and was rotated at 195.69 Hz (10 μs/channel). The chopper interrupts the flux of molecules leaving the Rh(111) surface at a distance of 10.5 cm from the electron impact ionizer.

It is possible to make three independent molecular beams in our machine. The center beam is in the plane defined by the detector rotation; the other two beams define a perpendicular plane. They are canted at 15° to the plane of the detector rotation, so that all of the beams overlap at the position of the crystal. The crystal can be lowered out of the beam path, and the detector rotated so that the incident velocity distribution and intensity of the center beam can be directly measured.

The Rh crystal was cut to within 1° of the (111) plane, determined by Laue X-ray back-reflection. The crystal was cleaned by $Ar^+$ ion sputtering (~5 μA at 900 K), followed by annealing at 1300 K. Carbon was removed from the sample by exposing the 900 K surface to an $O_2$ beam followed by annealing at 1300 K for 3 min, which results in the removal of both surface and sub-surface oxygen. Cleanliness and surface flatness could be checked by Auger electron spectroscopy and He atom scattering.

During these experiments, we used a continuous beam of $NO_2$ (Matheson, 99.5%) and, when we wanted the surface free of oxygen, a continuous beam of $H_2$. By controlling the relative flux of the two beams, we were able to keep the surface nearly oxygen free during the course of the experiments. Oxygen coverage could be checked by titrating off adsorbed oxygen with an $H_2$ beam at surface temperatures $T_s \geq 650$ K while monitoring the signal of desorbing $H_2O$. This result could be calibrated by comparison with the $H_2O$ from a saturation coverage of oxygen deposited using $O_2$ dosing, 0.5 monolayers (ML). For the $NO_2 + H_2$ experiments reported in this paper, the oxygen coverage was less than 0.04 ML.

To determine the velocity distributions for the NO produced at the surface, the measured signal

has to be corrected for the contribution from scattered $NO_2$, which is partially cracked in the electron bombardment ionizer. If the cracking pattern is known, it is possible to make this correction by taking two spectra, one with the mass spectrometer tuned to a mass-to-charge ratio ($m/e$) of 30, and a second with $m/e=46$. A direct measurement of the $NO_2$ beam gave a value of 0.82:1; the ratio was expected to be greater than 2:1 [16]. This is probably due to some dimerization of the $NO_2$ to $N_2O_4$ (although no signal was detected at $m/e=92$), which is more stable at the temperature and pressure of the beam, typically 5 psia through a 100 μm nozzle at 300 K [17,18]. In fact, some larger clusters might be possible since the normal freezing point of $NO_2$ is 262 K, much higher than the internal temperature of our beam. When the direct beam is blocked by a shutter, molecules can still effuse into the main chamber after several collisions with the walls of the differential pumping regions. The TOF spectrum of this effusing gas at $m/e=46$ was fit by a Maxwell–Boltzmann velocity distribution with $\langle E\rangle=36$ meV instead of the 51 meV expected at the temperature of our source. Further, it was possible to increase the NO:$NO_2$ intensity ratio in the mass spectrometer by using rare gas seeded beams and low stagnation pressures, when clustering is less likely. These results indicate that at least some of incident gas is $N_2O_4$ and possibly larger clusters.

That we do not know the exact cracking ratio is not a problem for the $NO_2+H_2$ experiments, due to the low amount of $NO_2$ signal relative to NO signal, and so should have a very small effect on our results. This is shown in Fig. 1, where a 1:1 ratio was used for the NO:$NO_2$ ratio from cracking in the ionizer. For the results at 60° and 75°, where there is a distinct tail at long times due to NO produced from scattered $NO_2$, the ratio could be, at most, 1.3–1.4:1 only if there were no contribution from the NO signal due to the surface decomposition of $NO_2$.

## 3. Results

Fig. 1 shows $m/e=30$ TOF spectra for the $NO_2+H_2$ reaction at $T_s=800$ K. The circles are the result of deconvolving the raw data from the cross-correlation pattern. The lines are the result of using a nonlinear least-squares fitting routine, convolving shifted Maxwell–Boltzmann velocity distributions:

$$f(v)\propto v^3\cdot\exp\left[-\left(\frac{v-v_0}{\alpha}\right)^2\right], \tag{1}$$

with the flight time broadening due to the finite length of the ionizer ($v$ is the velocity, and the three fitting parameters are the intensity, $v_0$, and $\alpha$). The solid line is the sum of all of the contributions to the $m/e=30$ TOF spectra. To arrive at these results, a spectrum with the mass spectrometer tuned to $m/e=46$ had to be taken at each angle. This was fit with the sum of two shifted Maxwell–Boltzmann velocity distributions; the results are the two broken lines with the lowest intensities. (As mentioned, we have used a 1:1 NO:$NO_2$ fragmentation). The long dashed line is the computed result for the product NO from the surface reaction using the same values of $v_0$ and $\alpha$ for all of the spectra. The average values are 315 meV for $\langle E\rangle$ and 1360 m/s for $\langle v\rangle$. For comparison, a Maxwell–Boltzmann velocity distribution ($v_0=0$ and $\alpha^2=2k_bT_g/m_g$, where $k_b$ is Boltzmann's constant, $T_g$ is the temperature of the gas, and $m_g$ is the mass of the gas molecule) at $T_g=800$ K, what you might expect for desorbing molecules equilibrated to the surface temperature has $\langle E\rangle=138$ meV.

The points shown in Fig. 2 are the average energies for the surface produced NO at the surface normal and $T_s$ from 500 K to 1000 K. The line through the points is simply a cubic fit to aid the eye. Also shown is a line for what would be expected for the barrierless desorption of the molecules if they were equilibrated to the surface temperature; the measured energies are much higher. Interestingly, for the lower surface temperatures, the slope of the energy versus $T_s$ function is greater than $2k_b$, indicating a stronger dependence of the final translational energy than expected for surface accommodation. A common method for characterizing the width of a velocity distribution is the speed ratio:

$$\mathrm{SR}=\sqrt{\left(\frac{\langle v^2\rangle}{\langle v\rangle^2}-1\right)\Big/\left(\frac{32}{9\pi}-1\right)}, \tag{2}$$

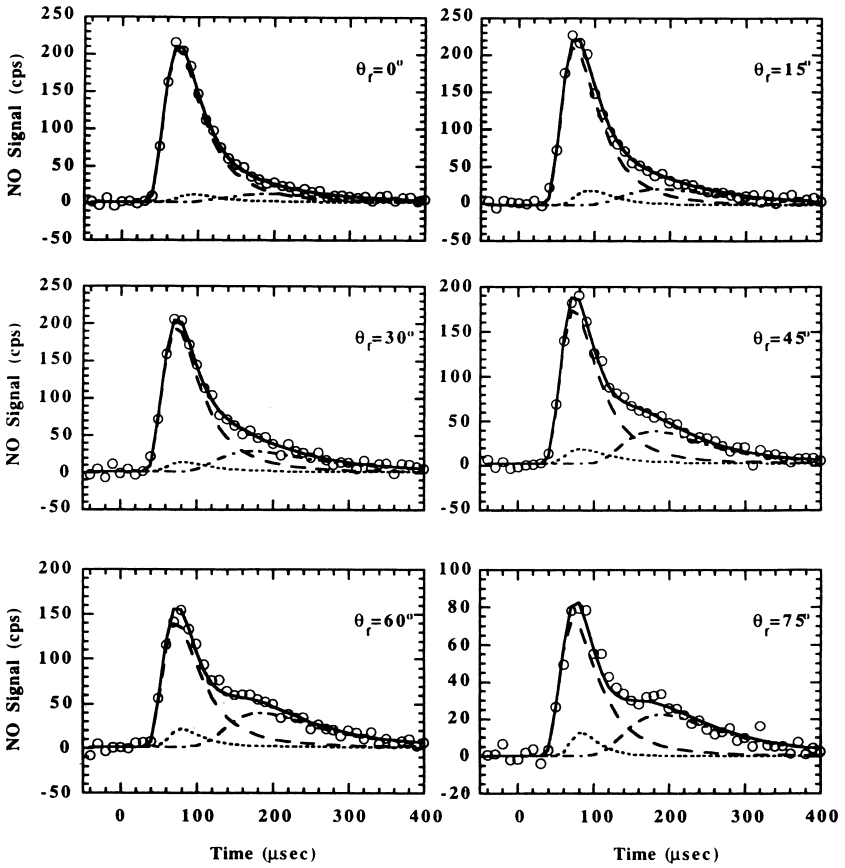


Fig. 1. NO TOF spectra at different final angles for the $NO_2+H_2$ reaction on Rh(111), with $\theta_i=45^\circ$ and $T_s=800$ K. The circles are the data after deconvolving from the cross-correlation pattern. The two lowest intensity broken lines are fits to the signal from $NO_2$ fragmentation; the other dashed line is the estimate for the surface produced NO; the solid line is their sum.

which compares the width of the measured velocity distribution with that of a Maxwell–Boltzmann distribution with the same average energy. For the results shown in Fig. 2, this ratio varies from about 0.83 to 0.92, narrower than a Maxwell–Boltzmann, with distributions measured for higher surface temperatures having on average a larger speed ratio.

Fig. 3 shows the intensity of the surface produced NO as a function of detector angle, normalized to the value at the surface normal, for three values of $T_s$. The solid line is for a $\cos(\theta_f)$ distribution, and the dashed line is for an intensity distribution that varies as $0.43\cos^{2.8}(\theta_f)+0.57\cos(\theta_f)$, derived from a fit to the data taken at $T_s=600$ K, which appears to be slightly peaked towards normal. For the higher temperatures, the angular dependence of the intensities is cosine within our error. At both $T_s=600$ K and 800 K, the measured velocity distributions are independent of final angle.

The hydrogen prevents oxygen from accumulating on the surface, and $H_2O$ is produced on the surface. We looked at the $H_2O$ product TOF spectrum at $T_s=800$ K. The result is fit by a Maxwell–Boltzmann velocity distribution cooler (733 K) than $T_s$, which agrees with our previous results for the $H_2+O_2$ reaction on Rh(111) [19]. NO also decomposes to nitrogen and oxygen on Rh(111). At $\theta_f=0^\circ$ and $T_s=800$ K, we were able to detect a very small amount of very high energy $N_2$, but too little for decent statistics to be accumu-

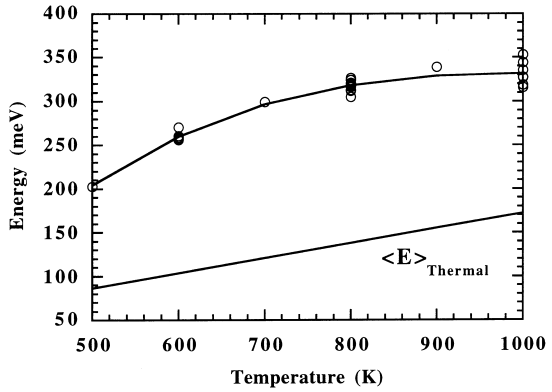


Fig. 2. Average energies for NO produced from the $NO_2+H_2$ reaction as a function of surface temperature. The solid line through the points is a cubic fit to aid the eye, the other solid line is what would be expected if the NO had equilibrated and desorbed with a thermal Maxwell–Boltzmann velocity distribution at the surface temperature.

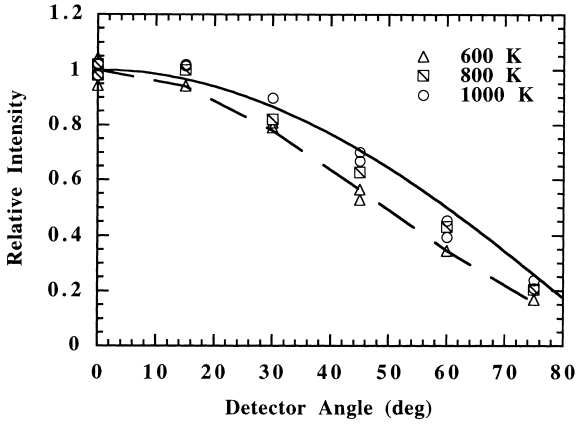


Fig. 3. Relative NO product intensity, normalized by the value at the surface normal, from the $NO_2+H_2$ reaction as a function of final angle probed for three different surface temperatures. The solid line is $\cos(\theta_f)$, and the dashed line is $0.43*\cos^{2.8}(\theta_f)+0.57\cos(\theta_f)$.

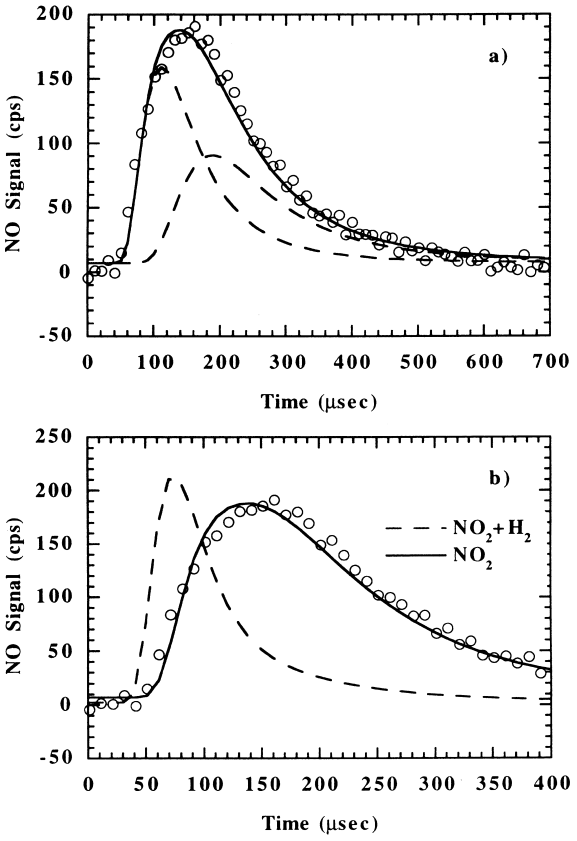


Fig. 4. NO TOF spectrum at $\theta_f=0°$ for the decomposition of $NO_2$ on Rh(111) after oxygen has been allowed to accumulate taken at $\theta_i=45°$ and $T_s=800$ K. The circles are the data after deconvolving from the cross-correlation pattern. (a) The lowest intensity broken line is a fit to the signal from $NO_2$ fragmentation; the other dashed line is the estimate for the surface produced NO; the solid line is their sum. (b) The same data, compared to the fit of the spectrum for the $NO_2+H_2$ reaction taken at $\theta_f=0°$ and $T_s=800$ K.

lated without prohibitively long counting times; we did not further investigate this channel. The TOF spectra were identical to those we had measured for the $NO+H_2$ reaction [3]. It is possible that there was some NO in the $NO_2$. However, our results from the experiments with NO showed that the probability of reaction was small, so it is doubtful that the majority of the $N_2$ we see could be due to the decomposition of NO in the incident $NO_2$ beam.

Fig. 4a shows an $m/e=30$ TOF spectrum measured at the crystal normal and with $T_s=800$ K when there was no $H_2$ beam. For these data, the crystal was exposed to $NO_2$ for $\sim$2 min before starting data collection, allowing oxygen to build up. We did not measure the amount of oxygen at the end of the experiment, but from our knowledge of oxygen desorption, there is at least $\sim$0.5 ML of adsorbed and absorbed oxygen at this temperature. The integrated intensity, as measured by a

counting ratemeter, did not vary during the course of the experiment, so the dynamics were essentially invariant. Again, we had to measure a spectrum at $m/e=46$, but the results are well represented by a single shifted Maxwell–Boltzmann velocity distribution. The result is shown as the lower intensity broken line in Fig. 4a, with the intensity ratio for $NO:NO_2=1$. Relative to the experiments taken with reducing conditions, there is much more scattered $NO_2$ away from specular under these oxidizing conditions. The second dashed line is the expected result for a Maxwell–Boltzmann velocity distribution at the surface temperature ($\langle E\rangle=$ 138 meV). The solid line is then the sum of the two contributions. The product NO is notably less energetic than for NO produced on the oxygen-free surface. Fig. 4b clearly shows this; the dashed line is the fit to the spectrum taken at $\theta_f=0^\circ$, shown in Fig. 1. Within experimental uncertainties, the product NO energy is independent of $T_s$, and the angular intensity distribution is essentially cosine, or only slightly peaked towards normal.

Fig. 5 shows examples of the signal due to $NO_2$ scattered from the surface. Fig. 5a shows the results when the surface is exposed to $NO_2+H_2$ with $\theta_f=60^\circ$, and Fig. 5b shows results for just $NO_2$ at $\theta_f=0^\circ$, both measured at $T_s=800$ K. Incident $NO_2$ beam conditions, including the flux, were the same. As already mentioned, the amount of $NO_2$ scattered at angles away from specular is much greater after oxygen has been deposited on the surface. The spectrum shown in Fig. 5a was fit with the sum of two shifted Maxwell–Boltzmann velocity distributions while the spectrum in Fig. 5b was fit with only one. The low energy (long flight time) feature in Fig. 5a ($\langle E\rangle=76$ meV, $\langle v\rangle=$ 540 m/s) and the feature in Fig. 5b ($\langle E\rangle=74$ meV, $\langle v\rangle=520$ m/s) have nearly identical velocity distributions. For the $NO_2+H_2$ reaction, where we took data at several surface temperatures, the velocity distributions had average values of about 65–85 meV for $T_s$ from 600 K to 1000 K, with the energies being slightly greater at the higher surface temperatures. In all cases, this is much lower than expected for accommodation to the surface ($2k_bT_s$ varies from 103 meV to 172 meV for $T_s$ varying from 600 K to 1000 K). In fact, the energy is close to that of the incident beam, and the signal

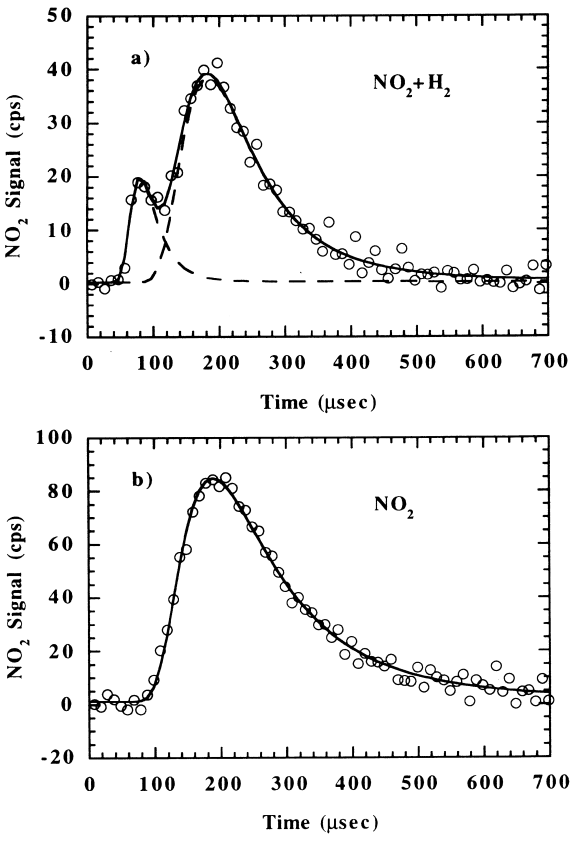


Fig. 5. (a) The scattered $NO_2$ signal for the $NO_2+H_2$ reaction taken at $\theta_f=60^\circ$ and with $T_s=800$ K. The data (circles) have been deconvolved with the cross-correlation pattern. The dashed lines are the two shifted Maxwell–Boltzmann velocity distributions and the solid line is their sum. (b) The scattered $NO_2$ signal when the surface is exposed to only the $NO_2$ beam at $\theta_f=0^\circ$ and $T_s=800$ K. The circles are the deconvolved data, and the solid line is the single shifted Maxwell–Boltzmann velocity distribution which fits the data.

is probably due to both elastic and inelastic scattering of the incident molecules.

The high energy feature in Fig. 5a is also fit with a shifted Maxwell–Boltzmann velocity distribution, but with $\langle E\rangle=392$ meV and $\langle v\rangle=$ 1245 m/s. For the data at $T_s=800$ K and 1000 K, the $\langle E\rangle\approx370$ meV, independent of the final angle investigated, and with the intensity somewhat peaked towards normal. For the data at $T_s=600$ K, $\langle E\rangle\approx250$ meV. However, the signal at all surface temperatures was weak and so these results are very approximate, though the difference

between $T_s = 600$ K data and the higher surface temperatures is real. At the present time, we have no explanation for this high energy feature, which occurs only under reducing conditions.

## 4. Discussion and conclusions

It is quite common that the products of surface reactions have high translational energies, and this is certainly true for the NO product from the $NO_2 + H_2$ reaction. In previous papers, we have used surprisal analysis in an attempt to discover the minimum number of parameters necessary to describe the dynamics [3,15]. For NO production at 800 K and 1000 K, where the angular variation of the intensity is cosine, the results can be reasonably described with the form:

$$f(v) = N\left[ v^3 \cdot \cos(\theta_f) \cdot \exp\left(\frac{-m_g^2}{2k_b T_s}\right)\right][\exp(\lambda v)]. \quad (3)$$

The first term in brackets, the prior distribution, is a Maxwell–Boltzmann velocity distribution at the surface temperature. The second term contains the single surprisal parameter, $\lambda$. This form gives nearly as good a fit (but a consistently larger value of $\chi^2$ from the least squares analysis) as the shifted Maxwell–Boltzmann distribution, and with one less parameter ($\lambda = 3.62 \times 10^{-3}$ s/cm at $T_s =$ 800 K). However, this way of examining the data adds little apparent insight. To attempt to interpret the data by detailed balance is more difficult, because the NO not only desorbs, but also dissociates. The second term in Eq. (3) can be viewed as a barrier to desorption, but the small value of $\lambda$ makes it very steep. It might be that the energy comes totally from the breaking of the N—O bond, but this is hard to rationalize with the strong surface temperature dependence of the translational energy.

Without an $H_2$ beam to remove the adsorbed oxygen from the decomposition of the $NO_2$, the translational energy of the product NO changes dramatically. Having a Maxwell–Boltzmann distribution at the surface temperature, it appears that we are measuring the desorption of fully accommodated molecules from a barrierless adsorption well. It is possible that the $NO_2 + H_2$ reaction has different dynamics, because the reaction is actually between adsorbed H and $NO_2$, rather than the H serving to remove oxygen from the surface. However, the NO product yield and translational velocity were independent of the $H_2$ flux, until it was too weak too remove all of the oxygen. Then the TOF spectra would begin changing, getting slower as the oxygen built up. In line with the results of the low temperature adsorption experiments on other transition metals, where the geometry of the adsorbed $NO_2$ changed in the presence of adsorbed oxygen, a more likely explanation is that the presence of oxygen changes the $NO_2$–surface interaction potential. That the surface potential is appreciably different is manifested by the increase in the direct-inelastically scattered component of the incident beam.

The principal findings are that for the $NO_2 + H_2$ reaction, the NO product has much more translational energy than expected for equilibration at the surface temperature, but is dependent on $T_s$. There is total energy scaling; the final energy is independent of final angle. The angular dependence of the NO intensity is nearly cosine for the higher surface temperatures, and peaked towards normal at $T_s = 600$ K. Also, it appears that some of the product NO decomposes to $N_2$ and oxygen. When the $H_2$ beam is turned off, oxygen builds up on the surface from the dissociation of $NO_2$. Under these oxidizing conditions, NO product has an approximately Maxwell–Boltzmann velocity distribution at $T_s$. These results add to our knowledge of $NO_x$ reduction on rhodium. They also show how the dynamics can be radically changed by the condition of the surface, depending upon whether the oxygen from the decomposition is allowed to build up or is continuously removed.

## Acknowledgements

Acknowledgment is made to the donors of The Petroleum Research Fund, administered by the ACS, for partial support of this research. This work was also supported, in part, by the AFOSR

and the Materials Research Science and Engineering Center Program of the National Science Foundation under awards DMR-9400379 and DMR-9808595. J.I.C. also thanks AT&T Bell Laboratories for financial support through the Graduate Research Program for Women.

## References

[1] K.C. Taylor, Automobile Catalytic Converters, Springer, Berlin, 1984.
[2] W.F. Egelhoff Jr., in: D.A. King, D.P. Woodruff (Eds.), The Chemical Physics of Solid Surfaces and Heterogeneous Catalysis, Elsevier, New York, 1982.
[3] J.I. Colonell, K.D. Gibson, S.J. Sibener, J. Chem. Phys. 104 (1996) 6822.
[4] B.A. Banse, B.E. Koel, Surf. Sci. 232 (1990) 275.
[5] D.H. Parker, M.E. Bartram, B.E. Koel, Surf. Sci. 217 (1989) 489.
[6] I.J. Malik, J. Hrbek, J. Vac. Sci. Technol. A 10 (1992) 2565.
[7] M.E. Bartram, R.G. Windham, B.E. Koel, Surf. Sci. 184 (1987) 57.
[8] D.T. Wickham, B.A. Banse, B.E. Koel, Surf. Sci. 223 (1989) 82.
[9] D.T. Wickham, B.A. Banse, B.E. Koel, Surf. Sci. 243 (1991) 83.
[10] U. Schwalke, J.E. Parmeter, W.H. Weinberg, J. Chem. Phys. 84 (1986) 4036.
[11] M.E. Bartram, R.G. Windham, B.E. Koel, Langmuir 4 (1988) 240.
[12] K.A. Peterlinz, S.J. Sibener, J. Phys. Chem. 99 (1995) 2817.
[13] K.D. Gibson, J.I. Colonell, S.J. Sibener, Surf. Sci. Lett. 343 (1995) L1151.
[14] D.F. Padowitz, S.J. Sibener, Surf. Sci. 254 (1991) 125.
[15] J.I. Colonell, K.D. Gibson, S.J. Sibener, J. Chem. Phys. 103 (1995) 6677.
[16] NIST, Chemical Name Search@http://webbook.nist.gov/chemistry.
[17] K. Jones, in: A.F. Trotman-Dickenson (Ed.), Comprehensive Inorganic Chemistry, Pergamon Press, New York, 1973.
[18] CRC Handbook of Chemistry and Physics, CRC Press, Boca Raton, 1986.
[19] K.D. Gibson, J.I. Colonell, S.J. Sibener, J. Chem. Phys. 103 (1995) 6735.